

Investigation of the heat distribution in dry friction systems during fade and recovery using fiber-optic sensing and infrared technology

Albert ALBERS, Thomas KLOTZ*, Chris FINK, Sascha OTT

IPEK–Institute of Product Engineering, Karlsruhe Institute of Technology, Baden Württemberg 76131, Germany

Received: 20 July 2020 / Revised: 09 October 2020 / Accepted: 12 March 2021

© The author(s) 2021.

Abstract: The design of dry-running friction pairings and systems determines not only their installation space and costs, but also their reliability under critical load conditions, for example in emergencies, in the case of faults, and in the event of misuse. While knowledge of the contact pattern is highly important for the development of clutches and brakes, the contact-related measurement of the temperature of these systems has not yet been solved in a satisfactory manner. Despite its importance, the temperature distribution has only been measured in a few studies. Typically, temperature measurements of complete clutches and brakes are carried out using thermocouples only. In this study, a new innovative test setup is presented. This setup is able to measure the heat distribution of the lining and the steel disk of a brake with high spatial resolution by means of fiber optic sensing technology and thermography. As a novelty, it enables measurement of the heat distribution and allows to correlate it with the fade and recovery behavior. Contrary to the expectations, the contact pattern is heterogeneous in circumferential direction. Possible causes are discussed using simulation results. Along with surface analysis, the new setup contributes to the investigation of the causes of fade and recovery.

Keywords: dry-running clutch and brake; fade and recovery; high-resolution spatial temperature distribution measurement

1 Introduction

The desire for an increasing performance and economy of the installation space and costs of clutches and brakes results in a demand for marginal dimensioning. The requirements of the friction and wear properties of friction pairings hence are continuously growing and can only be met through a precise comprehension of the tribological behavior. The tribological behavior of the friction pairings is constantly changing due to thermo-mechanical stresses in the tribological contact, resulting in phenomena like fade and recovery and leading to a lack of function and to poor comfort. Fading is described as a loss of brake efficiency under high thermal loads of 300–400 °C [1]. As a result, the

coefficient of friction decreases from its former tolerance field to a new state [2, 3]. By reducing the thermo-mechanical stresses in the subsequent synchronization cycles, it is possible to recover the coefficient of friction to its former higher level [2, 4–6]. However, the formation of a new state of equilibrium with reduced coefficient of friction is also possible [2].

The state of research offers various models which can be used to explain the volatile friction behavior during fade and recovery. The influence of the friction layer on the tribological properties is highlighted in many publications [7–10]. In addition, the effects such as tribo-oxidation [11–13], phase transition from solid organic material to gas or liquid [14, 15], and thermal phenomena [16] play a major role. For example, the

* Corresponding author: Thomas KLOTZ, E-mail: thomas.klotz@kit.edu

coefficient of friction of a new friction pairing changes during running-in due to establishing good conformity at the frictional surfaces [2, 4] and on account of the formation of the friction layer [3, 5, 6]. The friction layer is formed in the tribological contact under thermo-mechanical stress by the wear resistant ingredients of the friction lining and wear particles [9, 17]. According to Musiol and Poeste [5, 18], iron particles from the pressure plate are also deposited in the friction layer forming oxides. Thus, the chemical composition of the tribologically formed layer plays a key role regarding the wear and friction properties of dry friction systems [8, 9]. Referring to Eriksson and Jacobson [9], the contact situation of organic friction pairings is formed by primary and secondary plateaus transferring the friction forces. These plateaus are built up locally and destroyed at irregular intervals. Despite this dynamic mesoscopic situation, the friction and wear properties of the tribological contact are stable on the macroscopic scale [10]. Musiol [5] observes changes in the friction-force-transmitting areas as well, which can possibly be attributed to different mechanical and thermal stresses occurring locally. Ostermeyer [17] describes the processes in the friction layer as an equilibrium of the birth and death of the contact patches. If the thermo-mechanical stress in the tribological contact is increased and thus fading occurs, it can be assumed that the equilibrium of the contact patches is disturbed. More patches are destroyed than built up, hence the friction layer gets damaged and the coefficient of friction decreases [19]. Gopal et al. [4] estimate that the fading effect occurs because of the formation of a tribologically induced "film" consisting of particles from the organic lining and the pressure plate. Mechanical removal of the "film" regenerates the coefficient of friction [4].

Thermal phenomena like hot spots and hot bands also interact with wear particles [16]. Bulges in the tribological surface area are known for carrying higher frictional forces and therefore creating locally higher frictional heat [20]. Cristol-Bulthé et al. [16] have shown that wear particles get trapped in the open hollows of the waviness of the pressure plate. Thus, flat plateaus are formed in the areas of the high frictional heat and possibly stabilize the coefficient of friction.

Further studies focus on thermally induced reaction products of the friction lining components [14, 15, 21].

Fidlin et al. [15] study the fading effect by focusing on the degradation of the lining binder forming a pressure field in the tribological contact. As a result of the increasing gas pressure, the normal load is reduced and the transmissible torque decreases. Another possible explanation of fading is the decomposition of the resin forming lubricating substances [21]. Only a few models provide an explanation of the recovery. For example, it is possible to illustrate the increasing coefficient of friction by the decreasing thermo-elastic deformation of the pressure plate due to the lower frictional power insert at the end of a brake cycle [15]. Recovering the mean coefficient of friction over many cycles may be explained by the removal of the damaged friction layer and formation of a new layer with different friction and wear properties [5].

According to some of the presented models, local temperature differences affect the nature of the friction layer. Despite its importance, the temperature distribution has been measured in a few studies only. These include, for example, thermographic measurements of hot spots in railway disc brakes [22]. Quasi-direct measurements with a thermal camera show, that these temperature peaks are subject to constant movement. In long-term experiments they are even able to oscillate periodically [23, 24]. Consequently, two approaches to the measurement of the temperature distribution of the friction lining and the metal disk are available at the Institute of Product Engineering. With the first one, temperature measurements of ceramic friction materials have been done by Mitariu-Faller using infrared technology [25]. The second one uses fiber-optic sensing in order to measure the temperature distribution in the metal disk. Kniel et al. [26] developed its basic applicability and Weidler et al. [27] measured the temperature distribution in clutch components. Both studies show, for example, that the temperature distribution may have several maxima along the radius of the disk. Nevertheless, measurements of complete clutches or brakes are missing. In this paper, the temperature distribution close to the friction contact is measured with high spatial resolution by means of both, fiber optic sensing technology and thermography, in order to get a deeper understanding of the mechanisms occurring in the tribological contact.

2 Experimental setup and procedure

An industry brake with a mass pressed organic friction lining and low-alloyed steel plates is investigated. The lining is metal-free and reinforced by short glass fiber. The material composition of the lining is shown in the cross-section, see Fig. 1. Based on the energy-dispersive X-ray analysis, various fillers such as barium sulfate, silicon dioxide, and chopped glass fibers are recognized in its rubber-containing matrix. Such fillers are known to improve the heat stability, the friction characteristics, and the comfort [28].

The permanent temperature durability of the friction lining is below 250 °C. Due to its high rubber and low metal content, it is likely to achieve good comfort properties [29]. It has a low thermal conductivity of below 1 W/(m·K) in contrast to the steel disk with 48 W/(m·K).

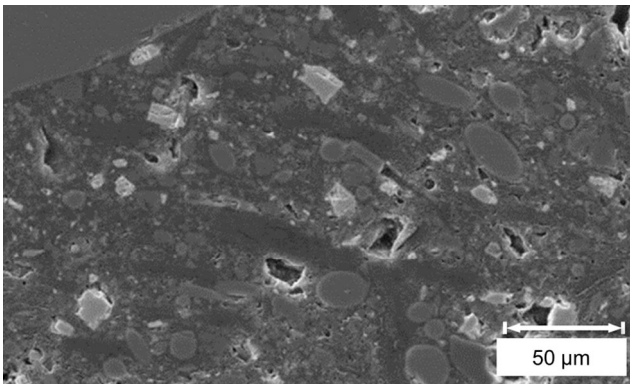


Fig. 1 Cross-section of the friction lining in the scanning electron microscope.

The setup is shown in Fig. 2. Using a real-time system, it simulates the brake process of a virtual flywheel by integrating the measured torque and calculating as well as regulating the rotational speed. During each brake cycle, the flywheel is initially accelerated to a defined rotational speed. The brake is then activated by no longer energizing its coil. Then, the springs of the brake press the two friction pairs with a previously set force. This brakes down the rotational speed of the flywheel until halt. The setup enables access to the temperature sensors on the backside of the brake. The thermocouples are optionally supplemented by the infrared camera IRCAM Equus 327kL pro filming through a hole in the steel plate or by the fiber optic sensor Luna ODiSI B. The fiber lies in eroded boreholes at a depth of 0.5 mm beneath the friction surface of the steel plate. Luna ODiSI B uses the Rayleigh scattering in order to measure the temperature. The fiber is irradiated by a laser.

The frequency pattern of the back scattering is measured by a detector. It embodies the characteristic fingerprint of the fiber, see Fig. 3. Increasing the temperature at a specific point of the fiber moves the characteristic pattern at this point. By evaluation of the movement of the characteristic pattern, it is possible to calculate the temperature change at this point [30]. In this study, the sensor spacing between these measuring points is 0.64 mm along the fiber at a frequency of 23.8 Hz. Further information on the functionality of the previous measurements can be found in Refs. [26, 30, 31]. In addition, wear is measured

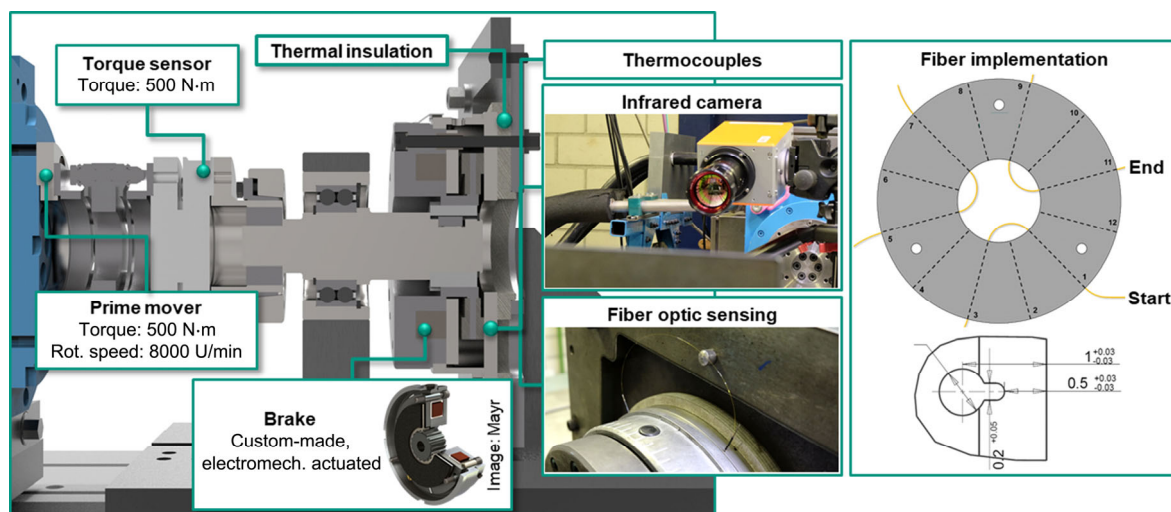


Fig. 2 Test setup brake with fiber optics and infrared technology.

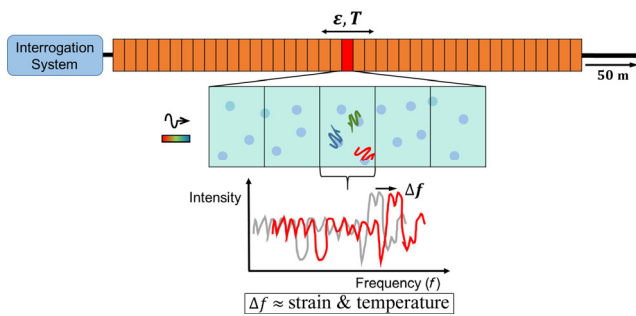


Fig. 3 Using Rayleigh scattering and converting its frequency shift in order to evaluate temperature or strain, redrawn from [31].

by weighing the components before and after the tests. The precision scale Kern PES 6200-2M with an accuracy of 0.01 g is used for the measurements.

Using this setup, the previously developed and published methods [32–34] are applied. After a running-in of 500 brake cycles each, several specimen of the friction pairing are used to determine and identify the brakes fade limit under short-term highly-increased load and to analyze its recovery under different conditions [33]. According to the manufacturer, the steel disk is phosphate-coated and protected by a preservation layer when new. Therefore, the running-in is performed in two stages. It starts with a specific friction work of 0.7 J/mm², which is increased to 1.3 J/mm² after the first 100 brake cycles. In the actual test, the rotational speed is highly increased for just one out of 25 brake cycles. This procedure is used to simulate emergency braking. In cooperation with the developers of clutches and brakes for industrial applications, it was decided to design it in this way. According to their experience, this test corresponds more to the real stress of these systems than, for example, the tests described in Regulation 90 of the Economic Commission of Europe of the United Nations [35], in which the temperature is increased over several cycles in order to cause fade. The so-called reference level corresponds to the stress in normal operation and the fade level to the brake cycles with highly increased load over a short period of time. Based on the results of the previous studies [33, 34], a so-called recovery collective is used in some cases. It uses five cycles of continuous slip at a lower starting temperature of 40 °C immediately after the fade level in order to improve the recovery behavior. Table 1 shows the parameters of all stages. These

Table 1 Test parameters.

Parameter	T_{Start} °C	p_{Nom} MPa	v_{Slide} m/s	q_A J/mm ²	\dot{q}_A W/mm ²	t_{Slide} s
Running-in stage 1	80	0.54	3.9	0.7	0.7	—
Running-in stage 2	80	0.54	5.2	1.3	1.0	—
Reference level	80	0.54	5.2	1.3	1.0	—
Fade level	80	0.54	16.2	12.5	3.1	—
Constant slip	40	0.54	1.9	3.7	0.4	10

parameters are defined to cause fade during the fade level and not to cause fade during the other levels such as the reference level. The parameters of the reference level are therefore comparatively low and matched to the data sheet of the friction lining. Such loads may occur in the real applications of this brake. After testing, several sections of the tests are repeated using either fiber-optic sensing or thermography.

3 Results and discussion

The results are presented below. Also, the findings are interpreted and generalized with regard to the friction models.

3.1 Evaluation of friction and wear properties

The temporary fade limit is determined and identified in order to define the strain of the fade level. Figure 4 shows the results. In the upper left part Fig. 4(a), the specific strain and load of the reference levels R and the load levels L_x is shown. After a preconditioning and warm-up of 50 brake cycles, the load levels are run through in increasing order. Every 25th brake cycle (50, 75, 100, etc.), rotational speed is elevated. As a result, the load levels have a higher specific strain and load. All load levels, L_1 (brake cycle 50, 75, and 100), L_2 (brake cycle 125, 150, and 175), L_3 (brake cycle 200, 225, and 250), L_4 (brake cycle 275, 300, and 325), and L_5 (brake cycle 350, 375, and 400), are repeated three times each. From load level L_1 to L_5 , rotational speed is gradually increased. Between those load levels, only reference levels are used. The upper right part Fig. 4(b) shows the friction coefficients of the load and reference levels. At load level L_4 with 12.5 J/mm², the coefficient of friction drops to values of less than

0.3 in all three repetitions. This load level corresponds to the brake sequence numbers 275, 300, and 325. It is found that friction is extremely volatile under these conditions. The coefficient of friction does not only drop during the load levels, it also increases to high levels of approximately 0.44 during recovery. The sliding speed of the load levels is gradually increased. The temperature recordings are shown in the lower left part Fig. 4(c). The load levels can be clearly recognized by their increased maximum temperatures. The changes of the maximum temperatures in the reference levels are explained by changes of the contact pattern. For example, when more load is carried near the tips of the thermocouples, higher maximum temperatures are measured. In addition, the linear regression shown in the lower right part Fig. 4(d) reveals the correlation between the maximum temperatures and the coefficient of friction. For example, the coefficient of friction falls below 0.3 at maximum temperatures of about 330 °C. It was decided to use this load level as fade level for the following tests. Based on the results, it was decided to use L_4 with 12.5 J/mm² as the so-called fade level.

Recovery is analyzed using the reference level as well as the recovery collective with constant slip at

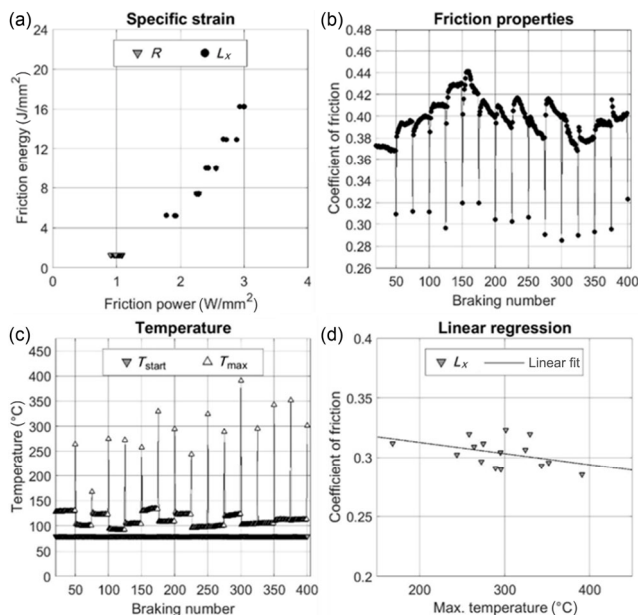


Fig. 4 Determination of the fade limit. (a) Specific strain of the reference and load levels with gradual increase; (b) coefficient of friction of each brake cycle with drops during the load levels; (c) start and maximum temperatures of each brake cycle with increase during the load levels; and (d) correlation between the maximum temperatures and the coefficient of friction.

40 °C. The advantage of the continuous slip is explained using Eqs. (1) and (2). According to Ref. [36], the specific frictional power \dot{q}_A is the product of the surface pressure p , the sliding speed v_{slide} , and the coefficient of friction μ . The specific frictional energy q_A results from the integration of the power over time.

$$\dot{q}_A = p \cdot v_{\text{slide}} \cdot \mu \quad (1)$$

$$q_A = \int \dot{q}_A dt \quad (2)$$

With a correspondingly low sliding speed and a high sliding time, the continuous slip allows to convert high loads of energy per brake cycle, see Table 1. Due to the low frictional power and the low starting temperature of 40 °C, the temperatures peak at a maximum of only 150 °C. As previously shown in Ref. [34], this allows recovery to be more reliable and to occur in a fewer number of brake cycles.

At first, the results are similar to the ones of the previous study [34]. The friction properties seem to scatter less and the transition duration seems to be shortened using the collective. In addition, a variance analysis is carried out for further comparison. This test is designed based on Ref. [37]. The design of experiments is done with the software Modde. Additionally, Matlab is used for analysis. In this test, the reference level and the recovery collective are repeated 30 times each in order to prove the difference based on statistical analysis. Figure 5 shows an excerpt of this test. It shows two examples of each variant, the reference level R and the recovery collective C. During the reference level, the coefficient of friction

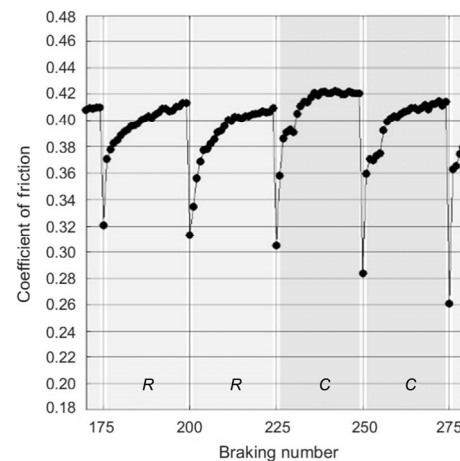


Fig. 5 Early excerpt of the comparison test.

rises slowly. In contrast, it rises faster using the constant slip of the recovery collective. In addition, it reaches slightly higher values towards its end.

Unfortunately, another effect is observed: The coefficient of friction drifts slowly to a level of approximately 0.3 during the whole duration of the test consisting of 1,625 brake cycles. Overall, this increases the variance of both variants. Therefore, the test does not lead to any statistically provable difference. The wear of the friction lining is assumed to be the cause of the loss of friction. The lining loses 13.77 g within the test. As a result, the friction lining loses thickness and thus the brake loses preload. In spite of the initially promising results, the statistical proof is not successful. As in this case, the variance analysis produces high amounts of wear due its length and high load. In retrospect, the load could have been reduced or brake systems with readjustments could have been operated in order to reduce the high wear and the drift effect. Nevertheless, carrying out such a test is important in order to obtain certainty about the effects of the changes. The applied setup and determination and identification of the temporary fade limit are reflected also. The experiment focuses on emergency braking with short-term, strongly increased stress, which is usually not examined at all. The methods may be very pragmatic and may also require further adjustments in order to be established as a standard test. The test setups may also be too complex and expensive. Nevertheless, knowledge of the fade limits under these conditions is crucial for many applications. For example, some friction pairings take over four times higher stresses in the short term without quickly wearing out while others fade quickly and wear out fast. Regarding dimensioning, huge

savings are possible using this knowledge.

3.2 Evaluation of thermal behavior

Selected episodes of the previous tests are repeated using the advanced temperature sensors. These tests start with the running-in from Table 1. After the fade levels, the reference levels and the recovery collectives are performed. The fiber optic measurement technology and thermal imaging camera provide new insights of the fade and recovery behavior of the brake. Figure 6 shows the heat distribution in the steel disk during the running-in. The temperature is mapped over the dimensions of the disk. Each of the six measuring sections contains 25 measuring points with a consistent distance of 0.64 mm. The temperature is interpolated between the measuring points. In brake cycle No. 10, the steel disk is still rather cold due to the lower specific friction work of stage 1 of the inlet. Nevertheless, it can be seen that the steel disk is warmer in its lower half. This is clearly visible in stage 2 of brake cycle No. 178. About 300 brake cycles later, changes in the contact pattern are observed. The warm area has become wider and the maximum temperature has decreased. In the lower area, however, the steel disk has stayed warmer. The contact pattern appears to change slowly in the running-in over many brake cycles.

In contrast, as a result of the fade level, significantly larger and faster progressing changes can be observed in Fig. 7. The contact patterns of the reference levels before and after fade differ clearly from each other.

It is remarkable, that no changes in the contact pattern are observed during recovery. Whether shortly after fade or 24 cycles later, the contact patterns are almost identical, see Fig. 8.

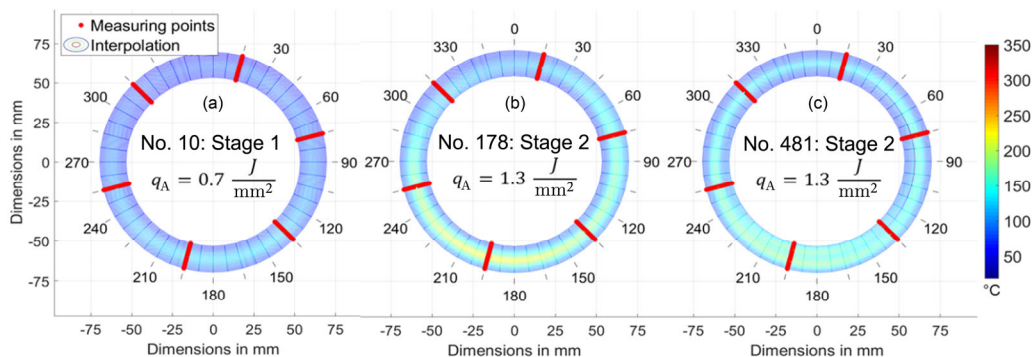


Fig. 6 High-resolution temperature measurement with fiber optics in (a) early; (b) mid; and (c) late brake cycles of the running-in.

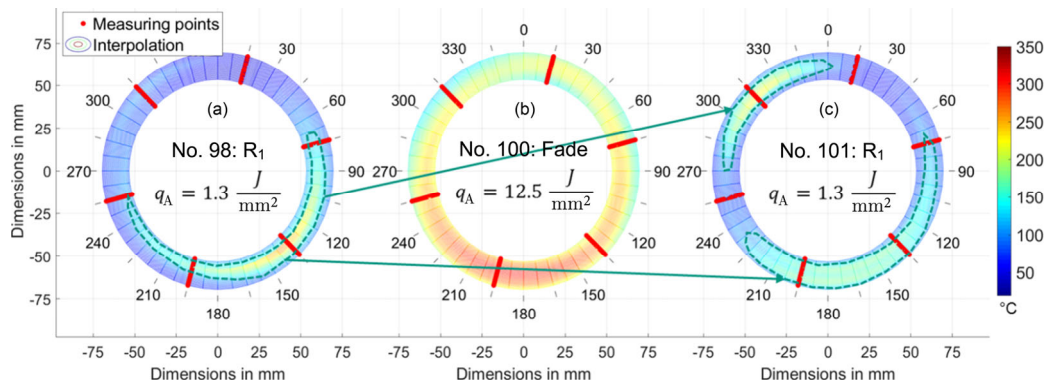


Fig. 7 High-resolution temperature measurement with fiber optics (a) before; (b) during; and (c) after fade.

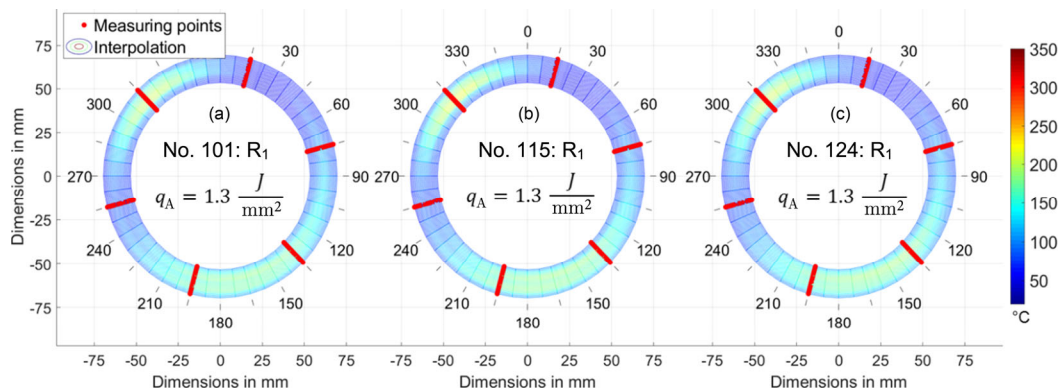


Fig. 8 High-resolution temperature measurement with fiber optics (a) five; (b) fifteen; and (c) twenty-four cycles after fade.

The heat distribution on the surface of the friction lining is measured using the infrared camera. However, due to the heterogeneous emission coefficient of the friction lining and changes in the tribological contact situation of the brake system due to the borehole, the results are subject to uncertainties. Because of this, deviations of ± 30 °C are expected using the infrared camera. In addition, this can change continuously due to changes in the roughness and the chemical composition of the surface during fade and recovery [33]. In purely qualitative terms, the results show that the contact pattern of the friction lining is heterogeneous as outlined by some of the presented models. Differences between the brake cycles before and after the fade levels could not be detected due to the rapid changes that already exist in a single brake cycle, see Fig. 9.

In contrast, the fiber-optic sensing is more precise: As described by Albers et al. [30], it has an accuracy of a few Kelvin, which depends on the geometry of the boreholes, the bending radius of the fiber, and the friction in the boreholes. Despite some inaccuracies in measurement, an uneven distribution of heat is

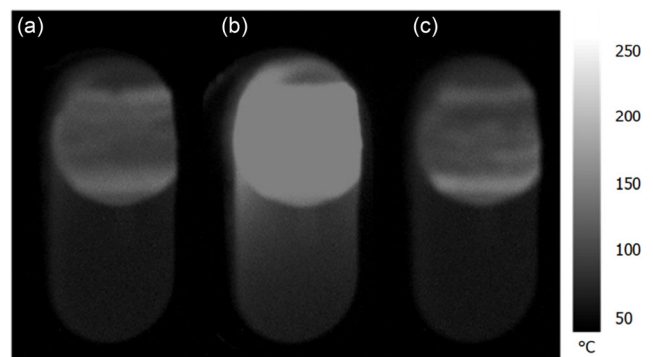


Fig. 9 Thermography measurement of the friction lining (a) before; (b) during; and (c) after fade.

observed using the fiber-optic sensing and the infrared camera. The distribution on the friction lining is apparently very fine-granular. That on the steel disk is coarser. The measurements are very complex, but they offer great potential for use in order to analyze contact patterns in future studies.

The results of the temperature measurements are compared with those from the state of research. However, this comparison is difficult due to the

different materials, geometries, and measuring techniques in each study. Compared to Refs. [23] and [24], the biggest difference lies in the periodic oscillations of the heat distribution. These changes between the inner and the outer ring could not be shown in the recent study. Compared to Ref. [22], the distribution of the hot spots is also irregular. The results are most similar to the ones of Kniel et al. [26] with the same fiber optic measurement technology. In these previous results, the unevenness is not noticeable due to its graphical representation. In some measurement data, however, there are differences of more than 100 °C along the circumference. Compared to the studies from the state of reasearch, the biggest advantage of the fiber optic measurement technology is noticable. It allows high-resolution measurements with only minor changes of the brake itself. The few eroded boreholes change the brake only slightly in comparison to other techniques such as Refs. [23, 24]. The thermography measurement, on the other hand, has the disadvantage of not being able to analyse the closed friction pairing. In this study, a major change, a hole in the steel plate, is required in order to see the friction lining.

Possible causes of the uneven contact pattern are discussed using a three dimensional finite element method simulation of a test bench with the same friction pairing with similar dimensions. The simulation is carried out in Abaqus. The integration of the thermal model is done with Matlab [38]. Heat conduction, convection, and radiation are mapped in it based on the model introduced by Merkel [39]. The surface of the steel disc is modeled with a stochastic distribution of elastic asperities [40]. For this purpose, the nodes of the surface are shifted in axial direction using a Matlab script. The distribution has a standard deviation of 1 μm . Their height is up to 3 μm . The values approximate the topography of the steel disk. Further, partitions with different element sizes are used in order to save computing time. Based on a convergence study, deviations in the maximum temperature of less than 5 °C are expected. Table 2 summarizes the assumed density ρ , the coefficient of thermal conductivity λ , the Young's modulus E , the heat capacity c , and the coefficient of thermal expansion ε of the materials.

Figure 10 shows the results of the simulation. The cross-sections explain why the temperature in the center of the friction surface is usually higher: At the

Table 2 Input parameters of the 3D FEM simulation.

Parameter	ρ	λ	E	ν	c	ε
Unit	kg/m ³	W/(m·K)	GPa	—	W/mm ²	1/K
Friction lining	2,020	1.1	0.42	0.42	0.501	6.86e ⁻⁵
Steel disk	7,280	48	210	0.24	470	1.5e ⁻⁵

edges, there is an additional heat flow in radial direction towards the outer areas. In the middle, however, the heat is only released in axial direction. In Addition, the asperities generate local increases in the surface pressure. In turn, these cause local differences in the distribution of heat. Comparing Figs. 8 and 10(c), the shape and size of the hot areas in the simulation look similar to the areas found in the temperature measurement.

The first results on this simplified simulation seem to explain the measured phenomenon. Slight differences in height seem to explain the differences of the temperature distribution. However, this is not necessarily the only cause. It is assumed that other mechanisms such as local differences of the friction layers or a misalignment of the disc also contribute to this. Even if the mechanisms are not fully understood yet, the temperature measurement makes an important contribution. It shows that the assumption of a point-symmetrical heat distribution is oversimplified. In circumferential direction, there are local differences of over 100 °C which must be taken into account in the design of clutches and brakes. The contact pattern of the steel disk is heterogeneous. Apart from that, it changes during running-in and fade. Thus, it presumably also has an influence on the frictional properties that change occurs during running-in and fade.

3.3 Evaluation of surface analysis

The friction surfaces are examined using a digital microscope as well as a scanning electron microscope (SEM) with energy-dispersive X-ray analysis. The samples are those of the tests with the shown test setup as well as the flywheel test bench from previous studies [33, 34, 41].

Figure 11 shows the steel plate and the friction lining of the brake. After running-in, both surfaces look evenly dull. The stressed area of the steel disk is only slightly darker than the rest. Immediately after the fade level, both surfaces are darker and shinier. Also,

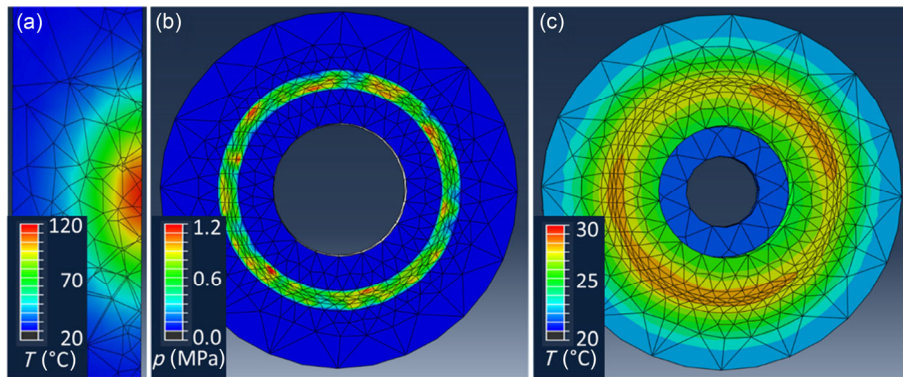


Fig. 10 Results of the 3D FEM simulation. (a) Temperature in the cross-section of the ideally smooth disk with rotationally symmetrical temperature distribution; (b) surface pressure with asperities; and (c) temperature of the surface with asperities after 14 s of cooling [38].



Fig. 11 Steel disk (top) and friction lining (bottom); after running-in (a, d); after fade (b, e); and after recovery (c, f).

dull areas are found on the friction lining. After the recovery level, the surfaces are again dull and even.

The dull areas are deeper regarding the topography of the lining. Also, large wear particles are found. They match with the valleys in terms of shape, see Figs. 12 and 13. When touched, these particles disintegrate

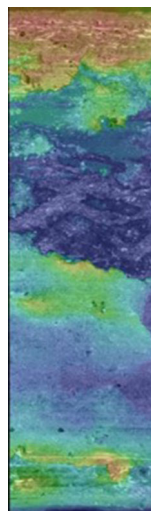


Fig. 12 Valley (blue coloring) in the topography of the friction lining with a maximum height difference of 93 μm.

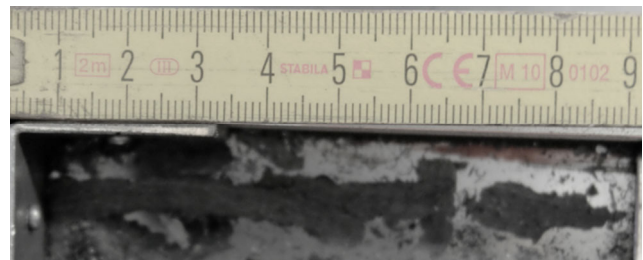


Fig. 13 Detached prolate plateau.

quickly. They consist of agglomerated wear particles. The new friction layer is prone to adhesive wear. Shreds of it easily peel off. Due to the high thermal load and outgassing of resin during fade, the cohesion of the matrix might be weaker than the adhesion in the friction contact. Therefore, friction is limited by cohesion. This friction layer gradually dissolves during recovery and is replaced by a new friction layer.

The two areas have different surface textures. In the shiny areas, mean arithmetic heights of $Sa = 3...14 \mu\text{m}$ are measured. The dull areas, on the other hand, are rougher with values of $Sa = 8...52 \mu\text{m}$. Also, the two areas show different microstructures, see Fig. 14. The

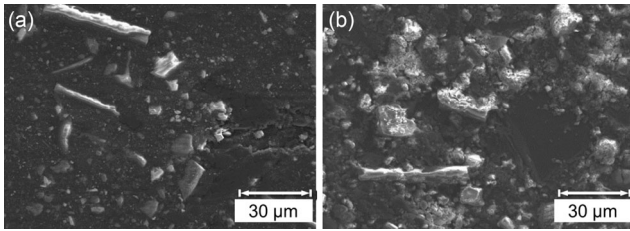


Fig. 14 SEM images of a (a) shiny and (b) dull area.

surface of the shiny areas also appears smoother in these SEM images.

It might be assumed that the metal like shine is produced by material transfer of iron from the steel plates. Comparing several areas, it is noticeable that the Fe content in the shiny areas is slightly higher, see Table 3. Nevertheless, its highest measured value is only 5.11%. The material transfer thus seems to take place in small quantities.

In addition, the friction linings are examined in order to compare their friction layers with the models from the state of research. Some areas fit very well with the Eriksson and Jacobson model [9]. Accordingly, secondary plateaus form at the side of some quartz particles, see Fig. 15(a). In addition, quartz particles with different plateaus are found. They are covered by these plateaus in Fig. 15(b). This behavior contradicts the Eriksson and Jacobson model [9]. According to this, the secondary plateaus form only on the side and not on top of the primary plateaus. The secondary plateaus are expected to widely disappear within the fade level. Instead, their formation is increased. Based on the Ostermeyer model [17], the increased occurrence of wear particles might contribute to this.

Table 3 Chemical composition of the shiny and the dull area.

Element	Weight percentage	
	Shiny area	Dull area
C	44.08	31.14
O	9.77	6.31
Mg	6.11	5.78
Si	1.47	1.43
Ca	2.06	2.93
Fe	0.77	0.00
Zn	31.46	46.31
Mo	4.28	2.87
Ba	0.00	3.23

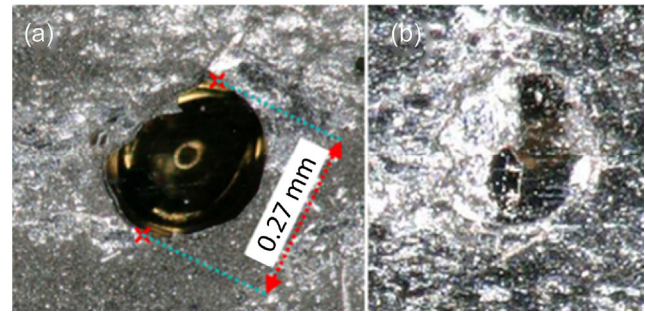


Fig. 15 Microscope images of (a) exposed and (b) covered quartz particles.

The large wear particles and the valleys can be explained with the Musiol model [5]. According to this, the particles are detached by local overuse. However, unlike found by Musiol, transfer of iron particles from the steel disk to the friction lining is only detected in small quantities. Compared to metal-containing linings, the friction lining causes low wear of the steel disk. Investigating other linings, this behavior can be observed in combination with the oxidation described by Musiol. Similar to what has been stated by Eriksson [9], plateaus of the friction lining are detached in order to analyze them from both sides. As described by Eriksson, these have a smooth top and a rough bottom, see Fig. 16.

It does not correspond with the current state of research that material transfers from the friction lining to the steel disk are detected repeatedly. It is suspected, that this has a certain impact due to its large size. Using the example of the brake, typical lining components are found on the steel disk. Figure 17 shows more examples coming from an industry clutch and different friction pairings using mass-pressed, wound, and sintered metal friction linings. The first example Fig. 17(a) also shows that adhesive wear occurs under

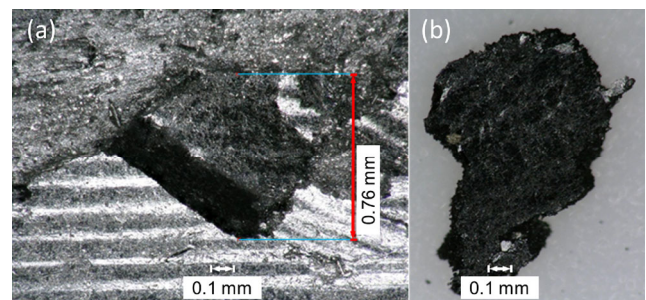


Fig. 16 Detached plateau with (a) a smooth and shiny upper side and (b) a rough and dull bottom side.



Fig. 17 More examples of material transfer. Pictures of (a, b) steel disks of mass pressed; (c) wound; and (d) sintered metal friction linings.

conditions with short-term highly-increased load. Material transfer creates distinct discoloration of the steel disks. Copper, for example, causes a reddish discoloration (Fig. 17(b)). Organic components (Fig. 17(c)) and sintered bronze (Fig. 17(d)) appear black due to oxidation. In the presented models, the steel disk is often depicted as a clean surface instead. Wear particles can stick to it [42] or get trapped in it [16].

On the whole, the third body layer is very similar to the Eriksson and Jacobson model [9], even though there are certain differences such as material transfer. Nevertheless, this does not prove the model, because the friction layer could, according to the Cristol-Bulthé et al. model [16], also form without primary plateaus. During fade, the friction level decreases. At the same time, gas formation is observed. This might explain the loss of friction in regard to the Fidler et al. model [15]. However, this is not clear yet because, according to Tanaka et al. [21], the reduced coefficient of friction can also be explained by the lubrication action of resin decomposition products. For this reason, there will be further tests with gas pressure measurement.

As shown in Fig. 4, friction might also be enhanced to high levels during recovery. Based on the Ostermeyer model [17], this can be explained with the increased third body formation due to higher occurrence of wear particles during and after the fade level. The local destruction of the third body layer can be described using the Musiol model [5]. It matches best with the valleys and wear particles found. Based on the changes in shine, changes of the friction layers microstructure are suspected. An influence of the material transfer of the friction lining on the steel disk is also suspected. It is shown, that this occurs in several friction pairings.

4 Conclusions

In this study, the previously presented methods [33, 34] were applied to a brake with a mass-pressed friction lining. For this purpose, a new test setup was developed. The fade limits could be confirmed on the basis of the investigations. Despite similar behavior, proof of the recovery collective's enhanced recovery was not possible due to the generally higher dispersion of the measurement results. With this new setup, measurements using the so-called fiber-optic measurement technology and a thermal imaging camera were carried out in order to investigate the distribution of heat. As a great innovation, the new setup enables the high-resolution temperature measurement of the frictional surfaces of a brake system. In circumferential direction, unexpected and huge temperature differences of over 100 °C are measured in the steel disk. These move during running-in and fade. The comparison with simulation results shows that these are probably caused by the topography of the steel disc. In the simulation, asperities with a height a few microns only create similar patterns. Surface and wear analyses were also carried out. The friction surfaces were examined by means of photo recordings, weight measurements, microscopic recordings, topography measurements, scanning electron microscopy (SEM), and energy-dispersive X-ray analysis. The findings were compared with the state of research. Despite deviations, the behavior can be described well with the existing models. As a complement to these models, material transfer from the friction lining to the steel disk seems to play an important role under such conditions with highly-increased load over a short period of time.

The aim of the study has been achieved, because it shows the contribution of the high-resolution temperature measurement regarding the investigation of fade and recovery. Nevertheless, further studies with new setups are planned in order to investigate and to differentiate between gas formation and lubrication action of resin decomposition products. Based on the quantitative description of these two effects, the modeling and understanding of fade and recovery behavior shall be further improved.

Acknowledgements

The authors thank for the support of the research project. The project 19377-N of the Research Association for Drive Technology is funded as part of the program for the promotion of industrial community research by the Federal Ministry for Economic Affairs and Energy on the basis of a decision by the German Bundestag.

Open Access This article is licensed under a Creative Commons Attribution 4.0 International License, which permits use, sharing, adaptation, distribution and reproduction in any medium or format, as long as you give appropriate credit to the original author(s) and the source, provide a link to the Creative Commons licence, and indicate if changes were made.

The images or other third party material in this article are included in the article's Creative Commons licence, unless indicated otherwise in a credit line to the material. If material is not included in the article's Creative Commons licence and your intended use is not permitted by statutory regulation or exceeds the permitted use, you will need to obtain permission directly from the copyright holder.

To view a copy of this licence, visit <http://creativecommons.org/licenses/by/4.0/>.

References

- [1] Bijwe J, Nidhi, Majumdar N, Satapathy B K. Influence of modified phenolic resins on the fade and recovery behavior of friction materials. *Wear* **259**(7–12): 1068–1078 (2005)
- [2] Lührs B. Wirkung der thermischen Belastung auf die Reibpaarungen großer Trommel- und Scheibenbremsen. Ph.D Thesis. Berlin (Germany): TU Berlin, 1987.
- [3] Gauger D. Wirkmechanismen und Belastungsgrenzen von Reibpaarungen trockenlaufender Kupplungen. Ph.D Thesis. Berlin (Germany): Technische Universität Berlin, 1998.
- [4] Gopal P, Dharani L R, Blum F D. Fade and wear characteristics of a glass-fiber-reinforced phenolic friction material. *Wear* **174**(1–2): 119–127 (1994)
- [5] Musiol F. Erklärung der Vorgänge in der Kontaktzone von trockenlaufenden Reibpaarungen über gesetzmässig auftretende Phänomene im Reibprozess. Ph.D Thesis. Berlin (Germany): Technische Universität Berlin, 1994.
- [6] Severin D, Gauger D. Leistungsgrenzen von Trockenkupplungen. Frankfurt am Main (Germany): Forschungsvereinigung Antriebstechnik e.V., 1996.
- [7] Rakowski W A. The surface layer of friction plastics. *Wear* **65**(1): 21–27 (1980)
- [8] Wirth A, Eggleston D, Whitaker R. A fundamental tribochemical study of the third body layer formed during automotive friction braking. *Wear* **179**(1–2): 75–81 (1994)
- [9] Eriksson M, Jacobson S. Tribological surfaces of organic brake pads. *Tribol Int* **33**(12): 817–827 (2000)
- [10] Eriksson M, Lord J, Jacobson S. Wear and contact conditions of brake pads: Dynamical in situ studies of pad on glass. *Wear* **249**(3–4): 272–278 (2001)
- [11] Dmitriev A I, Österle W, Kloß H. Numerical simulation of typical contact situations of brake friction materials. *Tribol Int* **41**(1): 1–8 (2008)
- [12] Buckley D H. *Friction, Wear, and Lubrication in Vacuum*. Washington (USA): National Aeronautics and Space Administration, 1971.
- [13] Kim S H, Lee H S. Effect of pressure on tribological characteristics between sintered friction materials and steel disk. *Int J Precis Eng Manuf* **12**(4): 643–650 (2011)
- [14] Herring J M. Mechanism of Brake Fade in Organic Brake Linings. In *Proceedings of the 1967 Automotive Engineering Congress and Exposition*, Detroit, USA, 1967.
- [15] Fidlin A, Bäuerle S, Boy F. Modelling of the gas induced fading of organic linings in dry clutches. *Tribol Int* **92**: 559–566 (2015)
- [16] Cristol-Bulthé A L, Desplanques Y, Degallaix G. Coupling between friction physical mechanisms and transient thermal phenomena involved in pad–disc contact during railway braking. *Wear* **263**(7–12): 1230–1242 (2007)
- [17] Ostermeyer G P. On the dynamics of the friction coefficient. *Wear* **254**(9): 852–858 (2003)
- [18] Poeste T. Untersuchungen zu reibungsinduzierten Veränderungen der Mikrostruktur und Eigenspannungen im System Bremse. Ph.D Thesis. Berlin (Germany): Technische Universität Berlin, 2005.
- [19] Ostermeyer G P. *Dynamik der Reibung in Bremsen*. Braunschweig (Germany): VDI-Berichte, 2002.
- [20] Barber J R. The influence of thermal expansion on the friction and wear process. *Wear* **10**(2): 155–159 (1967)

- [21] Tanaka K, Ueda S, Noguchi N. Fundamental studies on the brake friction of resin-based friction materials. *Wear* **23**(3): 349–365 (1973)
- [22] Panier S, Dufrénoy P, Weichert D. An experimental investigation of hot spots in railway disc brakes. *Wear* **256**(7–8): 764–773 (2004)
- [23] Dörsch S. *Periodische Veränderung Lokaler Kontaktgrößen in Reibpaarungen Trockenlaufender Bremsen*. Düsseldorf (Germany): VDI-Verlag, 2004.
- [24] Kleinlein C. *Beschreibung von Reibpaarungen in trocken laufenden Kupplungen und Bremsen durch ihre globalen und lokalen Reibungs- und Verschleißseigenschaften*. Baden-Baden (Germany): VDI-Verlag, 2006.
- [25] Mitariu-Faller M. Methods and processes for development of friction systems with advanced ceramics exemplified by dry running clutch systems for automotive. Ph.D Thesis. Karlsruhe (Germany): Karlsruhe Institute of Technology, 2009.
- [26] Kniel J, Gommeringer M, Lorentz B. A new approach for the optimization of the thermo-mechanical behaviour of dry-running clutches using fibre-optic sensing technology with high spatial measurement density. *Proc Inst Mech Eng, Part J: J Eng Tribol* **229**(8): 1003–1010 (2015)
- [27] Weidler A, Beitler H, Lassi S, Keller U. *Clutch protection function-clutch design one size smaller!?* Düsseldorf (Germany): VDI Verlag, 2017.
- [28] Chan D, Stachowiak G W. Review of automotive brake friction materials. *Proc Inst Mech Eng, Part D: J Autom Eng* **218**(9): 953–966 (2004)
- [29] Albers A, Ott S, Klotz T. *Abschlussbericht Kupplungsmodell III: Erholung Trockenlauf*. Frankfurt am Main (Germany): Forschungsvereinigung Antriebstechnik e.V., 2020.
- [30] Albers A, Ott S, Kniel J, Eisele M, Basiewicz M. Investigation of the thermo-mechanical behaviour of clutches using fibre optic sensing technology with high spatial measurement density. *Proc Inst Mech Eng, Part J: J Eng Tribol* **232**(1): 26–35 (2018)
- [31] Samiec D. Verteilte faseroptische Temperatur- und Dehnungsmessung mit sehr hoher Ortsauflösung. *Photonik* **6**: 34–37 (2011)
- [32] Klotz T, Ott S, Albers A. Experimentelle Ermittlung und Identifizierung der temporären Schädigungsgrenze trockenlaufender Friktionspaarungen. In *Proceedings of the 59th Tribologiefachtagung Reibung, Schmierung und Verschleiß*, Göttingen, Deutschland, 2018.
- [33] Klotz T, Ott S, Albers A. Analyse des Schädigungs- und Erholungsverhaltens trockenlaufender Friktionspaarungen. *Forsch Ingenieurwes* **83**(2): 209–218 (2019)
- [34] Klotz T, Bauer T, Ott S, Albers A. Synthese von Beanspruchungskollektiven zur Erholung trockenlaufender Friktionspaarungen und -systeme. In *Proceedings of the 60th Tribologiefachtagung Reibung, Schmierung und Verschleiß*, Göttingen, Germany, 2019: 182–190.
- [35] Information. https://unece.org/fileadmin/DAM/trans/main/wp29/wp29regs/R090r3e_01.pdf, 2012
- [36] VDI Fachbereich Produktentwicklung und Mechatronik. *VDI 2241 Blatt 1: Schaltbare fremdbetätigte Reibkupplungen und -Bremsen. Begriffe, Bauarten, Kennwerte, Berechnungen*. Düsseldorf (Germany): VDI Verlag, 1982.
- [37] Kleppmann W. *Versuchsplanung: Produkte und Prozesse Optimieren 8*. Hanser (München): Hanser-Verlag, 2013.
- [38] Wichmann S. *Modellierung des thermischen Verhaltens trockenlaufender Friktionspaarungen mittels der Finiten-Element-Methode am Beispiel des Trockenreibprüfstands*. M.Sc. Thesis. Karlsruhe (Germany): Karlsruhe Institute of Technology, 2018.
- [39] Merkel P. *Modelling of the temperature behavior and experimental investigations of the friction lining shape on the friction behavior on the example of dry running friction systems*. Ph.D Thesis. Karlsruhe (Germany): Karlsruhe Institute of Technology, 2016.
- [40] Greenwood J A, Williamson J B P. Contact of nominally flat surfaces. *Proc R Soc London. Ser A, Math Phys Sci* **295**(1442): 300–319 (1966)
- [41] Klotz T, Ott S, Albers A. Eine Methode zur Ermittlung der anwendungsspezifischen Leistungsgrenze trockenlaufender Friktionspaarungen. *Forsch Ingenieurwes* **83**(1): 11–20 (2019)
- [42] Ostermeyer G P. Friction and wear of brake systems. *Forsch Ingenieurwes* **66**(6): 267–272 (2001)



Albert ALBERS. He is a professor and head of IPEK–Institute for Product Engineering at Karlsruhe Institute of Technology (KIT), received his Ph.D. degree in mechanical engineering from Leibniz University Hannover, Germany, in 1987. Before

he started his position in Karlsruhe, he served as head of the Development Department and as deputy member of the executive board of a manufacturer of bearings, clutches, and gearboxes. His fundamental research philosophy is the simultaneous research on methods and processes of product engineering combined with the research on synthesis and validation

of new technical systems whilst taking into account the significant role of the engineer within the product development process. He and his team investigate methods to analyze future market requirements and the innovation process of new product generations in the following research areas: Drive systems and



Thomas KLOTZ. He is a research assistant at IPEK–Institute for Product Engineering at KIT, received his master degree in mechanical engineering from KIT, Germany, in 2016. Since then, he has been

working in IPEK’s research group Clutches and Tribological Systems. His research interests include the tribology and NVH of dry-running clutches and brakes, in particular the development of new test methods and setups for the investigation of fade and recovery.



Chris FINK. He is a student research assistant at IPEK–Institute for Product Engineering at KIT, received his bachelor degree in mechanical engineering from KIT, Germany, in 2018. Following on from his

bachelor’s thesis investigating the fade and recovery behaviour of dry-running friction systems, he joined the research group Clutches and Tribological Systems at IPEK. His field of activity includes the software implementation and experimental setup of the fiber-optic sensor.



Sascha OTT. He is a managing director of IPEK–Institute for Product Engineering at KIT and the KIT Center of Mobility Systems, obtained his degree in mechanical engineering from University of

Karlsruhe, Germany, in 2002. Beside of his current position, he serves as the head of the research fields clutches and brakes in drive systems and guides among others the research activities in the fields of drive systems, systems tribology, and validation of technical systems.